Stability of bound states near the zero-dispersion wavelength in optical fibers

David C. Calvo and T. R. Akylas
Department of Mechanical Engineering, Massachusetts Institute of Technology, Cambridge, Massachusetts 02139
(Received 14 May 1997)

The propagation of weakly nonlinear pulses near the zero-dispersion wavelength (ZDW) in optical fibers is governed by a modified nonlinear Schrödinger (NLS) equation with a third-order-derivative dispersive term. This equation is known to admit steady, multihump bound states that would require less peak power to launch than an ordinary NLS soliton pulse of comparable duration and with carrier wavelength in the anomalous dispersion regime. Here, the stability of the two-hump bound state for which third-order dispersion is most significant is examined. Linear stability analysis indicates the presence of a mild instability with $O(10^{-2})$ growth rate. Numerical solutions of the modified NLS equation, however, reveal that, under certain conditions, nonlinearity has a stabilizing effect, permitting two-hump pulses to propagate for long distances without collapsing. Depending on the type of perturbation, a perturbed bound state evolves to a neighboring state with carrier frequency shifted either towards or away from the ZDW. The evolution of more general pulse profiles near the ZDW is also considered and the effect of fiber loss is discussed. [S1063-651X(97)00810-6]

PACS number(s): 42.81.Dp

I. INTRODUCTION

The propagation of weakly nonlinear pulses in single-mode optical fibers is governed in general by the nonlinear Schrödinger (NLS) equation that combines the leading-order nonlinear and dispersive effects. The NLS equation admits envelope-soliton solutions with a ''sech'' profile when the carrier frequency of the pulse is in the anomalous dispersion régime. The peak power required to generate a NLS soliton is inversely proportional to the square of its width and directly proportional to the strength of the fiber dispersion at the carrier wavelength of the pulse. It would seem most efficient, therefore, to operate near the zero-dispersion wavelength (ZDW), the borderline between normal and anomalous dispersion, where dispersive effects are relatively weak [1]. This suggestion rests on the assumption, however, that one can in fact launch pulses with envelopes of permanent form, such that nonlinearity and dispersion are in perfect balance, near the ZDW in optical fibers.

At the ZDW, where the group velocity is stationary, the dispersive term of the NLS equation vanishes and a third-order-derivative dispersive term must be included in order to achieve a balance between nonlinear and dispersive effects. Unlike the NLS equation, however, no analytical envelope-soliton solutions of this modified NLS (MNLS) equation, that replaces the NLS equation near the ZDW, are available.

Based on asymptotic studies of the steady MNLS equation treating the third-order dispersive term as a small perturbation [2–5], it is now known that NLS solitons become nonlocal—they feature short-scale oscillatory tails with nonzero amplitude at infinity. Accordingly, when a pulse in the form of a NLS soliton is used as initial condition of the MNLS equation, short-scale oscillations are radiated, causing the pulse to decay as it propagates along the fiber [6], and schemes for absorbing the emitted radiation have been proposed [7]. Hence, when perturbed with a third-order dispersive term, NLS solitons do not survive, consistent with the claim that the MNLS equation does not accept locally confined solitary-wave solutions with a single hump [8].

It is interesting, on the other hand, that there exists an infinity of solitary-wave solution families of the MNLS equation featuring more than one hump. These solutions are possible in the anomalous dispersion régime at discrete values of the third-order dispersion. Specifically, two-hump solitary envelopes were found first, following a numerical search procedure [9]. From the numerical results it is seen that the spacing of the two humps increases as third-order dispersion becomes less important and, in the NLS limit, the wave profile approaches two well-separated NLS solitons. Hence, close to the NLS limit, the two-hump solitary-wave solutions of the MNLS equation may be viewed as bound states of two nonlocal NLS solitary waves pieced together so that their tails match smoothly [9,10]. Based on this interpretation, a systematic asymptotic procedure can be devised to construct locally confined, symmetric bound states of the MNLS equation featuring any number of humps greater than one [11]. The asymptotic results are consistent with numerical solutions of the MNLS equation [10,11].

In assessing the potential significance of multihump bound states in nonlinear fiber optics, it is important to inquire into their stability against perturbations. In prior work, this question was addressed via numerical simulations of the MNLS equation using two-hump bound states as initial conditions and monitoring their subsequent evolution along the fiber [10]. According to these simulations, two-hump bound states with appreciable third-order dispersion, after traveling stably for some distance, eventually broke down. On the other hand, close to the NLS limit where the two humps are weakly coupled, no such instability was observed.

Apart from direct numerical simulations, the stability question has been studied analytically by treating bound states as weakly interacting NLS solitary waves [12,13]. However, this approach cannot be relied upon to obtain quantitative results for bound states with closely spaced humps as is the case near the ZDW. Moreover, as pointed out in [11], even close to the NLS limit when the humps are far apart, the construction of steady bound states cannot be completely explained by merely superposing nonlocal soli-

tary waves so as to cancel the radiated oscillatory tails at infinity.

In the present paper, we examine in some detail the stability characteristics of the two-hump bound state of the MNLS equation that is found closest to the ZDW and for which third-order dispersion is most significant. Given also its relatively simple shape, this is perhaps the most relevant of all bound states to nonlinear pulse transmission near the ZDW. Through a combination of linear stability analysis and numerical simulations, it is demonstrated that, under certain conditions, this bound state can in fact propagate stably for long distances in the presence of perturbations.

II. STEADY BOUND STATES

The envelope of a nonlinear pulse near the ZDW of a single-mode optical fiber is governed by the MNLS equation [14]

$$E_z - i\,\frac{k_0''}{2}\,E_{tt} - \frac{k_0'''}{6}\,E_{ttt} + i\,\frac{n_2\omega_0}{c a_{\rm eff}}\,E^2E^* + \frac{\alpha}{2}\,E = 0, \quad (1)$$

where E stands for the electric field, z denotes the propagation distance along the fiber, t is the retarded time, n_2 is the Kerr coefficient, ω_0 is the carrier frequency, c is the vacuum speed of light, $a_{\rm eff}$ is the effective fiber core area, and α is the fiber loss coefficient. The coefficients k_0'' and k_0''' of the two dispersive terms in Eq. (1) are the second and third derivatives of the carrier wave number evaluated at the carrier frequency.

We shall use dimensionless variables throughout,

$$Z = \frac{|k_0''|}{T_0^2}\,z, \quad T = -(\operatorname{sgn} k_0''')\left(\frac{6|k_0''|}{|k_0'''|}\right)^{1/3} T_0^{-2/3} t,$$

$$A = \left(\frac{\omega_0 n_2}{|k_0''| c a_{\rm eff}}\right)^{1/2} T_0 E, \quad (2)$$

T_0 being a characteristic pulse duration. The MNLS equation (1) then takes the form

$$A_Z + i\beta A_{TT} + A_{TTT} + iA^2A^* + \Gamma A = 0, \quad (3)$$

where

$$\beta = -\frac{\operatorname{sgn} k_0''}{2}\left(\frac{6T_0|k_0''|}{|k_0'''|}\right)^{2/3}, \quad \Gamma = \frac{\alpha T_0^2}{2|k_0''|}.$$

The parameter β measures the relative significance of second-order dispersion near the ZDW: exactly at the ZDW, k_0'' vanishes and $\beta = 0$, while, in the other extreme, far from the ZDW where second-order dispersion dominates third-order dispersion ($T_0|k_0''| \gg |k_0'''|$), $|\beta| \gg 1$ and the NLS limit is recovered. The parameter Γ is a measure of losses in the fiber.

In discussing steady bound states, we set $\Gamma = 0$ and consider the effects of loss in a later section. Following the approach taken in [9], we first write

$$A = a(\xi, Z)\exp[i(\Omega\xi - KZ)], \quad (4a)$$

$$\xi = T - \nu Z, \quad (4b)$$

where a satisfies

$$-ia_Z + \overline{\beta}a_{\xi\xi} - \overline{K}a + a^2a^* + i\overline{\nu}a_\xi - ia_{\xi\xi\xi} = 0, \quad (5)$$

with

$$\overline{\beta} = \beta + 3\Omega, \quad \overline{K} = K + \nu\Omega + \beta\Omega^2 + \Omega^3,$$

$$\overline{\nu} = \nu + 2\beta\Omega + 3\Omega^2. \quad (6)$$

The parameters Ω and K amount to shifts in the carrier frequency and wave number, respectively, while ν allows for a shift in the speed of the envelope which, to leading order, propagates at the group speed corresponding to the carrier frequency.

It is convenient to normalize the envelope amplitude by rescaling variables according to

$$a = |\overline{K}|^{1/2}a', \quad \xi = |\overline{K}|^{-1/3}\xi', \quad Z = |\overline{K}|^{-1}Z' \quad (7)$$

so that, after dropping the primes, Eq. (5) becomes

$$-ia_Z + \lambda a_{\xi\xi} - sa + a^2a^* + iva_\xi - ia_{\xi\xi\xi} = 0, \quad (8)$$

where

$$\lambda = \frac{\overline{\beta}}{|\overline{K}|^{1/3}}, \quad v = \frac{\overline{\nu}}{|\overline{K}|^{2/3}}, \quad s = \operatorname{sgn}\overline{K}. \quad (9)$$

Concentrating on solitary-wave envelopes, we then seek special solutions of Eq. (8) such that $a = re^{i\theta}$ maintains a permanent form ($a_Z = 0$) and has limited duration:

$$r(\xi) \to 0 \quad (\xi \to \pm\infty). \quad (10a)$$

Moreover, without any loss, the condition

$$\theta_\xi \to 0 \quad (\xi \to \pm\infty) \quad (10b)$$

is imposed, absorbing into Ω a possible frequency shift at the solitary-wave tails.

It turns out [9] that Eq. (8) (with $a_Z = 0$) subject to the boundary conditions (10) defines a nonlinear eigenvalue problem, λ being the eigenvalue parameter; solitary-wave solutions are possible only at specific values of λ and $v = s/\lambda$ ($s\lambda > 0$). Corresponding to each eigenvalue there is in fact a one-parameter family of solitary-wave solutions of the MNLS equation: once the carrier frequency is specified by fixing Ω, it is clear from Eqs. (6), (7), and (9) that the envelope profile and speed are completely determined. Alternatively, fixing the envelope peak amplitude by choosing K determines the envelope profile completely, including the carrier frequency and the envelope speed.

We also remark that bound states near the ZDW, being eigenstates, are fundamentally different from NLS solitons for which both the peak amplitude and the carrier frequency may be specified independently. Moreover, the instantaneous frequency distribution associated with a bound state,

$$\theta_\xi = \frac{\operatorname{Re}\{a\}\operatorname{Im}\{a_\xi\} - \operatorname{Im}\{a\}\operatorname{Re}\{a_\xi\}}{|a|^2}, \quad (11)$$

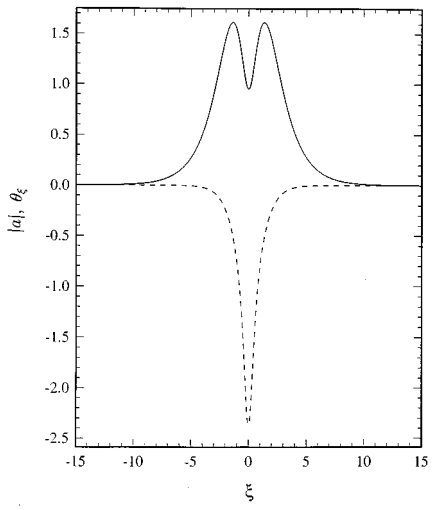

FIG. 1. Fundamental bound state: amplitude $|a|$ (—); instantaneous frequency θ_ξ (---).

varies throughout the wave profile, while it is constant [equal to zero according to the normalization (10b)] for a NLS soliton.

The discussion in this paper will focus on the stability of the two-hump bound state corresponding to the minimum eigenvalue $\lambda \equiv \lambda_0 = 2.4647$; this is the bound state closest to the ZDW and will be referred to as the fundamental bound state. The amplitude profile and instantaneous frequency distribution of the fundamental bound state are relatively simple in comparison to those of other multihump bound states, and are displayed in Fig. 1 as computed by a shooting procedure [9].

III. LINEAR STABILITY ANALYSIS

We first examine the stability of the fundamental bound state $a_0(\xi) = f(\xi) + ig(\xi)$ to infinitesimal perturbations. For this purpose, we write

$$a(\xi, Z) = a_0(\xi) + b(\xi, Z),$$

and upon substitution into Eq. (8), retaining terms linear in $b = p + iq$, the disturbance equation reads

$$-ib_Z + \lambda_0 b_{\xi\xi} - b + a_0^2 b^* + 2|a_0|^2 b + \frac{i}{\lambda_0} b_\xi - ib_{\xi\xi\xi} = 0. \tag{12}$$

Following the standard procedure, we then seek separable solutions of Eq. (12) in the form

$$\begin{Bmatrix} p \\ q \end{Bmatrix} = \begin{Bmatrix} P(\xi) \\ Q(\xi) \end{Bmatrix} \times \exp(\sigma Z), \tag{13}$$

where P and Q satisfy

$$(\sigma + 2fg)Q + \lambda_0 P_{\xi\xi} + (3f^2 + g^2 - 1)P - \frac{1}{\lambda_0} Q_\xi + Q_{\xi\xi\xi} = 0, \tag{14a}$$

$$(\sigma - 2fg)P - \lambda_0 Q_{\xi\xi} + (1 - 3g^2 - f^2)Q - \frac{1}{\lambda_0} P_\xi + P_{\xi\xi\xi} = 0. \tag{14b}$$

In the limit $|\xi| \to \infty$, f and $g \to 0$ since the underlying bound state is of limited duration, and the system (14) reduces to

$$\sigma Q + \lambda_0 P_{\xi\xi} - P - \frac{1}{\lambda_0} Q_\xi + Q_{\xi\xi\xi} = 0, \tag{15a}$$

$$\sigma P - \lambda_0 Q_{\xi\xi} + Q - \frac{1}{\lambda_0} P_\xi + P_{\xi\xi\xi} = 0. \tag{15b}$$

Hence,

$$\begin{Bmatrix} P \\ Q \end{Bmatrix} \sim \begin{Bmatrix} 1 \\ \mp i \end{Bmatrix} \times e^{\kappa\xi} \quad (|\xi| \to \infty), \tag{16}$$

where

$$\sigma = \left(\frac{\kappa}{\lambda_0} \pm i \right)(1 - \lambda_0 \kappa^2). \tag{17}$$

From Eq. (17), it is apparent that if κ is pure imaginary, σ has to be pure imaginary as well. Accordingly, for instability to be present (Re $\sigma > 0$), it is necessary that Re$\kappa \neq 0$ so the disturbance must be trapped close to the main pulse:

$$\begin{Bmatrix} P \\ Q \end{Bmatrix} \to 0 \quad (|\xi| \to \infty). \tag{18}$$

The equation system (14) subject to the boundary conditions (18) defines an eigenvalue problem for the parameter σ. It is important to note that if σ is an eigenvalue so are $-\sigma$ and σ^*. Hence the existence of a trapped disturbance is also a sufficient condition for instability, and the eigenvalue spectrum is symmetric about the Re σ and Im σ axes.

To search for trapped disturbances, the following numerical procedure was adopted. The system (14) together with the boundary conditions (18) were discretized using a fourth-order-accurate finite-difference method, and the spectrum of σ was first determined from the resulting matrix eigenvalue problem via a global eigenvalue solver. Once an initial estimate for the eigenvalues of interest had been obtained, the inverse power method with shifting was employed to improve the mode-shape resolution and the eigenvalue accuracy.

For the fundamental bound state, in addition to the continuous spectrum of neutral disturbances on the Im σ axis, a pair of eigenvalues is found on the Re σ axis at $\sigma = \pm 0.026$ corresponding to a trapped mode. From the amplitude distribution shown in Fig. 2, it is evident that this mode is only marginally trapped relative to the span of the bound state, and the instability develops over a long propagation distance as indicated by the small growth rate. This behavior is consistent with the roots κ of the dispersion relation (17) when given the growth rate σ. Specifically, there is a root corresponding to a short-scale oscillation that de-

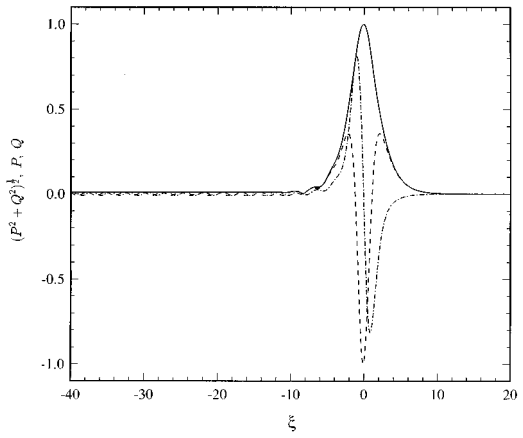

FIG. 2. Trapped mode with growth rate $\sigma=0.026$: amplitude $(P^2+Q^2)^{1/2}$ (—); real part P (–·–); imaginary part Q (---).

cays slowly for $\xi<0$, in agreement with the long tail seen behind the main peak in Fig. 2.

Apart from the modal analysis presented above, the possibility for linear instability was also explored by solving Eq. (12) numerically using a Gaussian initial condition with the same full width at half maximum (FWHM) as the fundamental bound state. For this purpose, a split-step Fourier spectral method was used, and the computational domain was expanded continually so as to avoid artificial reflections from its edges. As a check of the numerical procedure, it was verified that the conservation law

$$\frac{d}{dZ}\int_{-\infty}^{\infty}|b|^2 d\xi = i\int_{-\infty}^{\infty}(a_0^{*2}b^2 - a_0^2 b^{*2})d\xi,$$

which follows from Eq. (12), was satisfied. The evolution of the disturbance shown in Fig. 3 indicates that part of the initial perturbation disperses away, leaving a growing peak similar to the instability mode found earlier by the modal analysis. When in fact the exact shape of the unstable trapped mode was used as initial condition to Eq. (12), the numerically computed growth rate agreed well with that determined by the modal analysis.

Based on the linear stability analysis, therefore, the fundamental bound state is unstable to infinitesimal disturbances. The instability develops at a relatively slow rate, however, and it would be interesting to know how nonlinearity may affect the evolution of the disturbance. This question is addressed below by numerical simulations of the MNLS equation.

IV. NONLINEAR EVOLUTION

In solving the MNLS equation (3) numerically, the complex envelope $A(Z,T)$ is advanced in $Z>0$ by the symmetrized split-step Fourier method [14], starting with a given profile at $Z=0$ for $-\infty<T<\infty$. A prominent feature of the MNLS equation is the possibility of a resonance of the main nonlinear pulse with small-amplitude waves that manifests itself as radiation of an oscillatory tail propagating in the direction of $T<0$. Accordingly, as the pulse evolves, the left edge of the computational domain is closely monitored for incoming waves, and the entire domain is doubled to accommodate this radiation. The conservation law

$$\frac{d}{dZ}\int_{-\infty}^{\infty}|A|^2 dT = -2\Gamma\int_{-\infty}^{\infty}|A|^2 dT,$$

which follows from Eq. (3), serves as a check of the calculations.

We begin by solving the MNLS equation (3) without loss $(\Gamma=0)$ starting at $Z=0$ with the exact profile of the fundamental bound state so perturbations come only from the small truncation error in the numerical scheme. For convenience, the choice $\Omega=0$, $K=1$ is made, giving $\beta=\lambda_0$ according to Eq. (9). Although the fundamental bound state is linearly unstable, numerical simulations over long distances $(Z=1000)$ showed that only a small amount of radiation was being emitted in the direction of $T<0$, the main pulse propagating stably without any sign of breakup. Hence it appears that nonlinear effects provide a stabilizing action. This is in

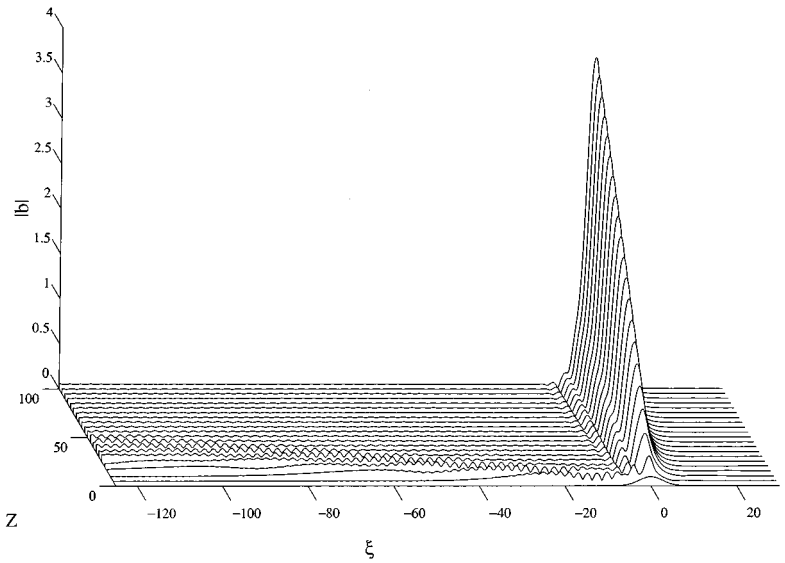

FIG. 3. Unstable evolution of an infinitesimal initial disturbance to the fundamental bound state.

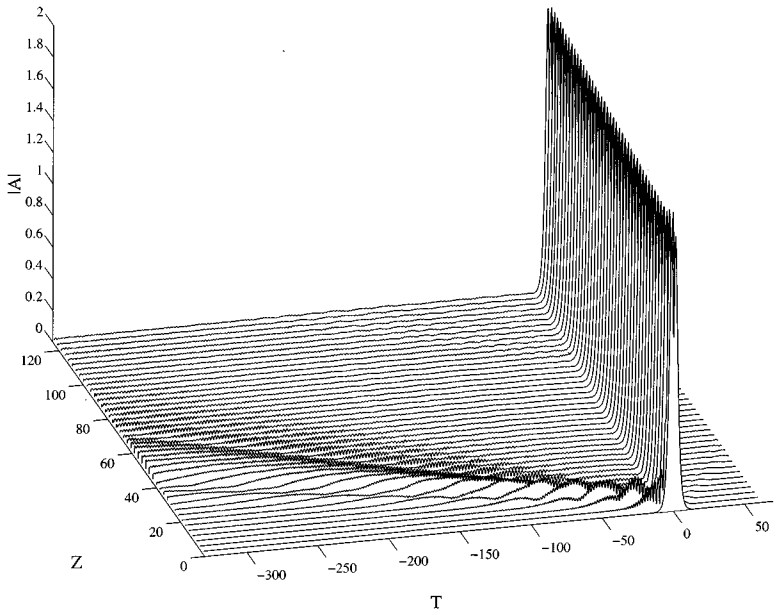

FIG. 4. Evolution of the fundamental bound state under a Gaussian disturbance at $Z=0$ with amplitude of 0.14.

contrast to the results presented in [10] where two-hump bound states with closely spaced humps were found to be unstable, rapidly collapsing after propagating a distance of $Z\approx 100$ along the fiber.

A. Amplitude perturbations

To gain further insight into the role of nonlinearity in curtailing linear instability, we now explore the evolution of the fundamental bound state under the same conditions as above ($\Omega=0$, $K=1$; $\beta=\lambda_0$) but in the presence of finite perturbations. Keeping the phase and hence the instantaneous frequency distribution intact, we add a Gaussian perturbation to the amplitude with the same FWHM as the unperturbed state. The evolution of the pulse for a perturbation amplitude of 0.14 is shown in Fig. 4. After an initial adjustment period ($Z\lesssim 15$) during which energy is radiated mostly in the direction of $T<0$, the pulse reaches a more or less stable form similar to, but not quite the same as, the unperturbed bound state. Specifically at $Z=130$, the pulse amplitude shows an increase from 1.615 to 1.804 and the FWHM decreases from 6.454 to 5.993 as shown in Fig. 5. These changes in amplitude and width are in accordance with the scalings (7) of steady bound states for $|K|=1.248$. We also remark that at $Z=130$ the instantaneous frequency of the pulse, as defined in Eq. (11), experiences a shift of about 0.06 at the tails of the envelope from its initial value of zero. Note that, for the fundamental bound state with $|K|=1.248$, Eq. (9) gives $\beta=\lambda_0|K|^{1/3}=2.653$ and, from Eq. (6), it follows that $\Omega=(\beta-\beta)/3=0.063$, consistent with the frequency shift found at the tails of the pulse. Moreover, the wave speed of the pulse at $Z=130$ is in excellent agreement with the steady-state value computed from Eqs. (6) and (9) for $|K|=1.248$.

In response to the amplitude perturbation, therefore, the pulse drifts towards a neighboring bound state with carrier frequency shifted away from the ZDW and hence with increased dispersion relative to the unperturbed bound state. This seems reasonable considering the fact that a bound state achieves a balance between nonlinear and dispersive effects: the increase in amplitude should come with a commensurate increase in dispersion.

As the amplitude of the initial perturbation is increased, however, the capacity of the pulse to adjust and approach a neighboring bound state diminishes. This is illustrated in Fig. 6 for an initial perturbation amplitude of 0.15; while some adjustment takes place initially, an instability eventually develops that overtakes the pulse over a distance of 75–100 units of Z. Therefore the fundamental bound state shows conditional stability to amplitude perturbations: as long as the initial perturbation amplitude is below a certain threshold, a perturbed fundamental bound state evolves towards a neighboring state and can propagate for long distances without collapsing. Clearly, nonlinearity plays an important part during this adjustment but, given that the fundamental bound

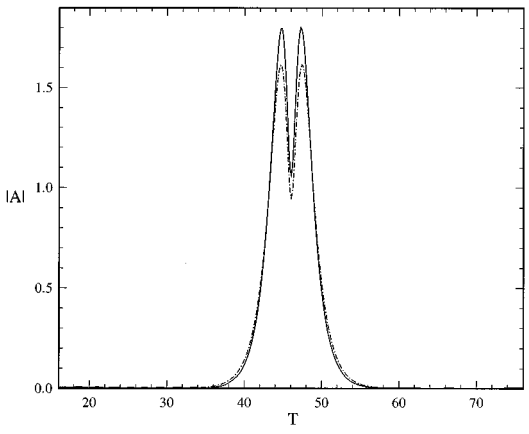

FIG. 5. Comparison of profile at $Z=130$ (—) against unperturbed profile (– · –) of the fundamental bound state under a Gaussian initial disturbance at $Z=0$ with amplitude of 0.14.

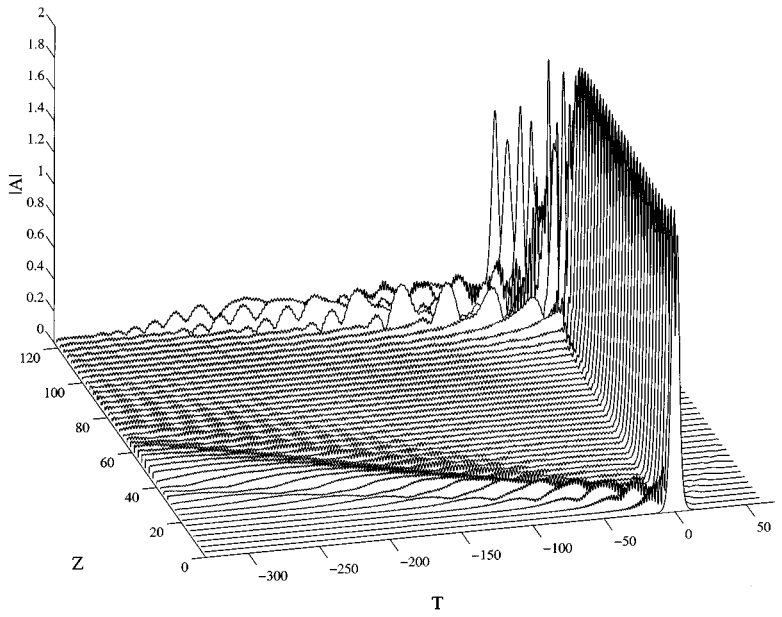

FIG. 6. Evolution of the fundamental bound state under a Gaussian disturbance at $Z=0$ with amplitude of 0.15.

state is unstable to infinitesimal perturbations, an entirely steady state cannot be approached.

B. Phase perturbations

As noted earlier, unlike NLS solitons, the envelopes of bound states near the ZDW have a variable frequency distribution or ''chirp.'' Since this feature apparently keeps the two humps bound together, it is useful to know how sensitive the pulse structure is to perturbations in the instantaneous frequency. For this purpose, we now explore the evolution of the fundamental bound state (with $\Omega=0$, $K=1$; $\beta=\lambda_0$) in $Z>0$ when at $Z=0$ it is perturbed by a constant frequency shift Ω'.

Numerical results for $\Omega'=-0.064$ are shown in Fig. 7. During $0<Z\lesssim 10$, the pulse radiates a part of its energy as it evolves to a state of lower total energy with a peak amplitude of 1.57 and a pulse width of 6.57. Once again, these changes are consistent with the scalings (7) of steady bound states ($|K|=0.94$) but here $\beta<\beta$, indicating that the pulse has evolved into a state closer to the ZDW where dispersive effects are weaker. When $\Omega'\lesssim -0.065$, however, the pulse cannot adjust to the frequency shift and breaks up over a distance of $Z\approx 50$, suggesting again that the fundamental bound state is only conditionally stable to frequency downshifts. On the other hand, when a frequency upshift ($\Omega'>0$) is imposed at $Z=0$, the pulse breaks up over a short distance even for very small Ω'.

Furthermore, we find qualitatively the same behavior if at $Z=0$ we allow for more general disturbances to the instan-

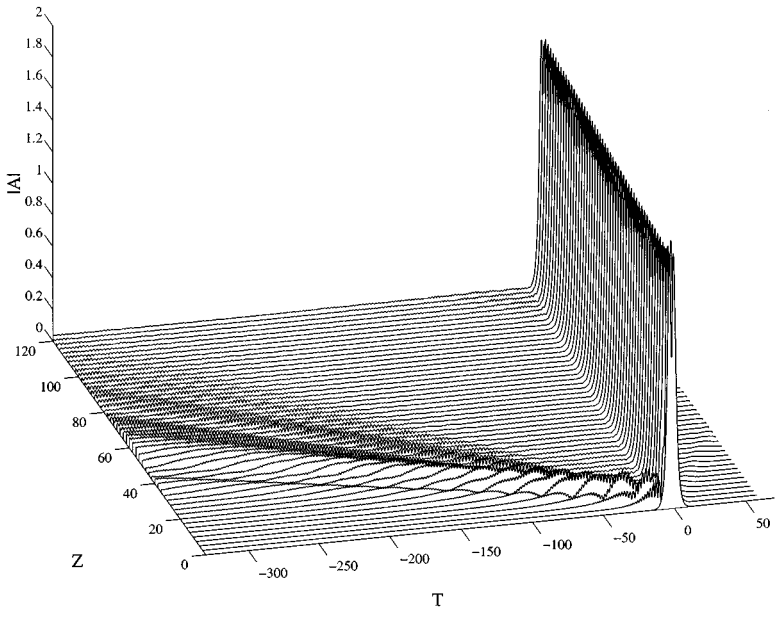

FIG. 7. Evolution of the fundamental bound state under a frequency shift $\Omega'=-0.064$ at $Z=0$.

taneous frequency of the fundamental bound state. In the presence of a Gaussian perturbation, for example, the pulse appears to evolve towards a state of lower total energy if the minimum instantaneous frequency is decreased by 10% but collapses over a distance of $Z \approx 90$ when the frequency is decreased by 15%. As before, any upshift in frequency away from the ZDW results in rapid instability and breakup.

This behavior can be understood intuitively by noting that as the carrier frequency of the pulse is shifted away from the ZDW, steady bound states require a higher peak amplitude because of the increased second-order dispersion. A higher peak amplitude would in turn require an increase in the total pulse energy, however, so the pulse cannot adjust to a frequency upshift. In contrast, when a frequency downshift is imposed, second-order dispersion becomes less important so a steady bound state requires less energy, which the pulse can accommodate by radiating small-amplitude dispersive waves.

C. More general initial profile

Based on the results presented thus far, it is concluded that if the amplitude and phase of the fundamental bound state are slightly distorted the pulse may propagate stably under certain conditions. From a practical standpoint, however, it may be difficult to tailor both the pulse shape and phase exactly, and it is desirable to know how far from an exact bound state the initial profile can be if a stable shape is to evolve.

In an attempt to address this issue, we now consider the evolution of a pulse whose amplitude distribution initially is quite different from that of the fundamental bound state. Specifically, we solve the MNLS equation taking the amplitude profile at $Z=0$ to be a Gaussian with roughly the same width as the fundamental bound state (with $\Omega=0$, $K=1$) and the phase to be close to that of the exact state but with a slight frequency upshift at the left tail. In the dimensionless variables of Eq. (3), the initial envelope profile is expressed as

$$A(T)=1.7\exp(-0.067T^2)\exp(-i\Theta),$$

where

$$\Theta(T)=1.49\tan^{-1}(\sinh 1.76T)-1.24\,\mathrm{erf}[0.4(T+5.25)].$$

When the MNLS equation (3) is solved subject to this initial condition, again with the choice $\beta=\lambda_0$, $\Omega=0$ and neglecting loss, the result is shown in Fig. 8. Over a very short distance, a depression forms in the middle of the pulse leaving two well-defined peaks. As the pulse adjusts to this change some energy is radiated, and over a distance of $Z \approx 10$ the pulse transforms into a shape closely resembling that of a two-hump bound state in both amplitude and instantaneous frequency. Even though this shape is not completely stable—an instability develops near $Z=45$ that eventually overtakes the pulse—the same Gaussian pulse without a phase modulation at $Z=0$ would evolve into a continuously radiating single peak rather than the quasisteady two-hump profile obtained here. Note that, for a carrier wavelength 0.3 nm away from the ZDW in pure silica where the group-dispersion coefficients take the values $k''=-0.035\ \mathrm{ps}^2/\mathrm{km}$ and $k'''=0.074\ \mathrm{ps}^3/\mathrm{km}$ [15], and with the choice $\beta=\lambda_0$ so $T_0=3.8$ ps according to the scalings used in Eq. (3), the dimensionless distance $Z=45$ corresponds to about 19 000 km.

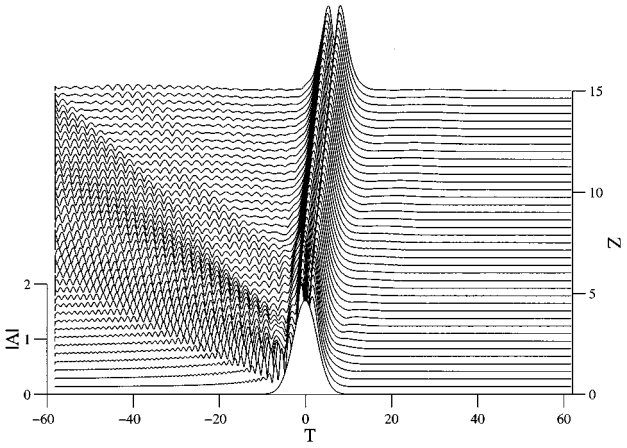

FIG. 8. Evolution of a pulse which at $Z=0$ has a Gaussian amplitude profile and phase close to that of the fundamental bound state.

Based on this numerical experiment, it would appear feasible to form a pulse resembling a two-hump bound state that may propagate for a considerable distance, as long as the initial profile retains some features of a bound state. The fact that a phase modulation can have a stabilizing influence in the presence of third-order dispersion was also recognized in [7], where it was shown that trains of single-hump pulses could be stabilized by applying a proper phase modulation. However, this study was concerned with the case of weak third-order dispersion while the results presented here are for strong third-order dispersion.

V. DISCUSSION

The present study has focused on the fundamental two-hump bound state for which third-order dispersion is most significant. From a practical standpoint, the relatively stable behavior of this pulse is favorable since, for a given pulse duration, the fundamental bound state can exist closest to the ZDW and hence has the lowest peak-power requirement in comparison with all the other bound states. The required peak power may be computed from Eqs. (2), (7), and (9) as a function of carrier wavelength and a_{eff} [14]. For instance, if once again a carrier wavelength 0.3 nm away from the ZDW is chosen, the peak power to generate the fundamental two-hump bound state turns out to be about one-third of that required to launch a NLS soliton with duration comparable to one of the humps at the threshold for radiation ($\beta \approx 4$). Thus considerable savings in power can be attained operating close to the ZDW.

On the other hand, it is important to ask how dissipation will affect pulse propagation near the ZDW. It is known that in the presence of relatively weak dissipation a NLS soliton undergoes a gradual change in amplitude and width as it loses energy [14]. To determine whether loss is a weak perturbation to the MNLS equation (3), the coefficient Γ may be computed. Specifically, for a carrier wavelength 0.3 nm

away from the ZDW and using the value $\alpha = 0.05\ \mathrm{km}^{-1}$ for the fiber loss coefficient which can be obtained for a dispersion-shifted fiber [16], the normalized loss is $\Gamma \approx 10$. In view of the fact that the nonlinear and dispersive terms in Eq. (3) are $O(1)$, loss is clearly not a weak perturbation to the MNLS equation and in this case pulses are expected to suffer a significant attenuation over a relatively short distance.

In practice, a judicious choice of the carrier wavelength (which also fixes the peak amplitude of a bound state) must take into consideration the waveguide dispersion relation at hand and the minimum loss attainable in a given situation. It is possible that a distributed amplification scheme such as Raman gain could possibly work well with the fundamental pulse considered here. In fact, it has been demonstrated that, in the absence of large disturbances, the fundamental pulse can propagate over a long distance. The benefits of using Raman gain depend of course on the amount of power required to excite the Raman process compared with the savings in power gained by operating close to the ZDW. As these loss-related issues require further study, they will not be pursued here.

In an actual waveguide, some fluctuation in the group-dispersion coefficients is expected and hence it is useful to determine how stable the pulses are to variations of this sort. Based on the frequency perturbations considered earlier (see Sec. IV B), we can obtain a rough idea of what might be expected in practice. The frequency downshift $\Omega' = -0.064$, for instance, results in an effective second-order dispersion of $\beta = 2.275$ according to Eq. (6), and, at a carrier wavelength 0.3 nm away from the ZDW, this value of β corresponds to 11% decrease in $|k''|$ which would normally occur over a wavelength range of 0.05 nm in pure silica. As mentioned before, the pulse will radiate a part of its energy for a decrease in $|k''|$ but will completely collapse for any increase in $|k''|$. Therefore, from a systems standpoint, loss and variations in the group-dispersion coefficients present the most formidable obstacles to transmission.

Finally, we note that contrary to the arguments in [13], the fact that bound states are eigensolutions does not necessarily suggest that they are inherently unstable. While it is true that solitary-wave solutions of Eq. (8) do not form continuous families in the parameter λ, when we consider Eqs. (4)–(7), it is clear that a bound state corresponding to an eigenvalue may physically assume a continuous range of energies depending on the carrier frequency. The results presented in this study suggest that the carrier frequency may shift towards or away from the ZDW depending on whether perturbations induce, respectively, a loss or gain in pulse energy. This adjustment, however, appears to occur only when changes are not too drastic. The relatively stable behavior of the fundamental two-hump bound state demonstrated in this study certainly warrants further experimental and theoretical investigations of pulse propagation near the ZDW.

ACKNOWLEDGMENT

Effort sponsored by the Air Force Office of Scientific Research, Air Force Materials Command, USAF, under Grant Numbers F49620-95-1-0047 and F49620-95-1-0443.

[1] P. K. A. Wai, C. R. Menyuk, H. H. Chen, and Y. C. Lee, Opt. Lett. **12**, 628 (1987).
[2] P. K. A. Wai, H. H. Chen, and Y. C. Lee, Phys. Rev. A **41**, 426 (1990).
[3] H. H. Kuehl and C. Y. Zhang, Phys. Fluids B **2**, 889 (1990).
[4] V. I. Karpman, Phys. Rev. E **47**, 2073 (1993).
[5] R. Grimshaw, Stud. Appl. Math. **94**, 257 (1995).
[6] P. K. A. Wai, C. R. Menyuk, Y. C. Lee, and H. H. Chen, Opt. Lett. **11**, 464 (1986).
[7] I. M. Uzonov, M. Gölles, and F. Lederer, Phys. Rev. E **52**, 1059 (1995).
[8] P. S. Jang and D. J. Benney, Dynamics Technology, Inc. Tech. Report No. DT-8167-1, 1981 (unpublished).
[9] T. R. Akylas and T.-J. Kung, J. Fluid Mech. **214**, 489 (1990).
[10] M. Klauder, E. W. Laedke, K. H. Spatschek, and S. K. Turitsyn, Phys. Rev. E **47**, R3844 (1993).
[11] D. C. Calvo and T. R. Akylas, Physica D **101**, 270 (1997).
[12] A. V. Buryak and N. N. Akhmediev, Phys. Rev. E **51**, 3572 (1994).
[13] A. V. Buryak, Phys. Rev. E **52**, 1156 (1995).
[14] G. P. Agrawal, *Nonlinear Fiber Optics* (Academic, San Diego, 1995).
[15] D. Marcuse, Appl. Opt. **19**, 1653 (1980).
[16] B. J. Ainslie, K. J. Beales, D. M. Cooper, C. R. Day, and D. J. Rush, Electron. Lett. **18**, 842 (1982).